SUPPLEMENTARY INFORMATION

Photophysical properties of PMI-COOH in organic solvents. The photophysical properties of this newly proposed membrane probe were tested in solvents with a broad range of dielectric constants. Except for water (which will be discussed later), very small shifts of the absorption maxima can be observed by increasing the solvent polarity (figure 1S), suggesting a combination of a small dipole moment of the molecule in the ground state with a larger dipole moment in the excited state. The large excited state dipole moment is confirmed by the red shift of the emission maxima in polar solvents (figure 1S). Furthermore, the fact that the absorption maxima do not systematically display a monotonous bathochromic shift upon increasing the solvent polarity (table 1S) suggests that solvent polarizability also influences the photophysical properties of PMI-COOH. The fluorescence lifetime remains around 4 ns in all solvents used. In alcohols, the fluorescence decay has to be analyzed as a sum of two exponentials. A small contribution (less than 5%) of a rise component observed at long wavelengths could be due to solvent relaxation phenomena. Similar data were obtained for Bodipy derivatives (1).

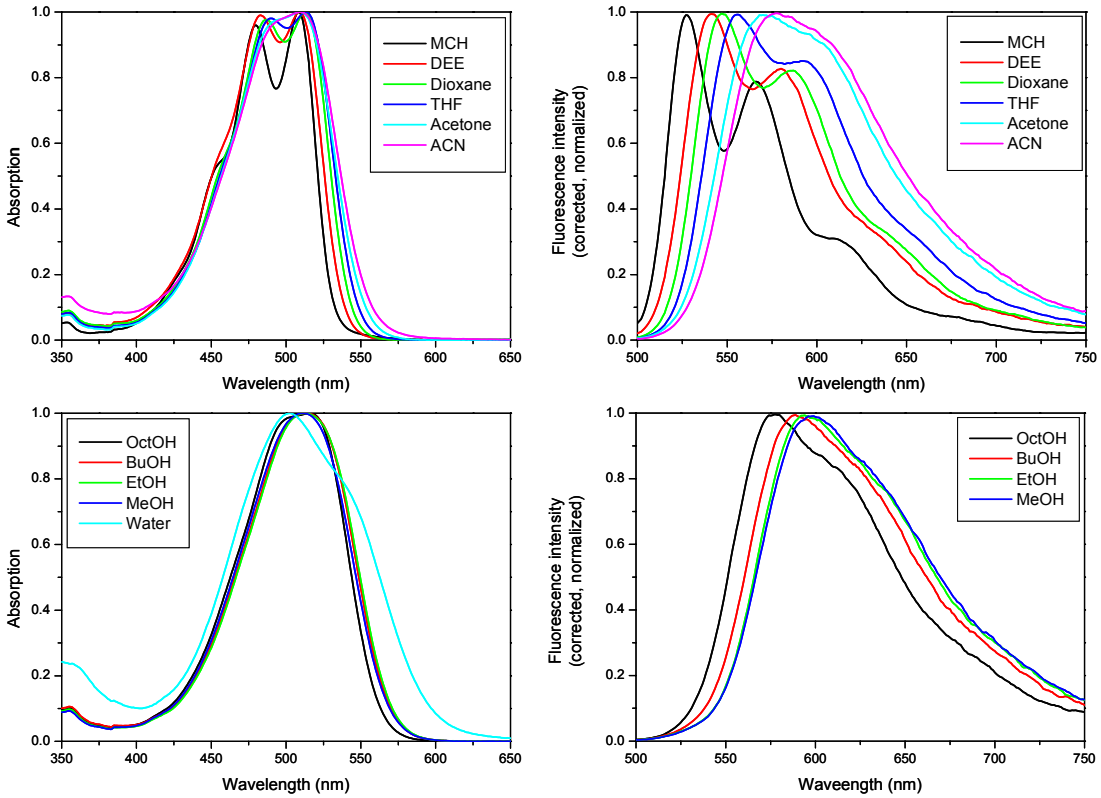

Figure 1S. Absorption (*left*) and emission (*right*) spectra (excitation at 488 nm) of PMI-COOH in different organic solvents (MCH = methylcyclohexane; DEE = diethylether; THF = tetrahydrofuran; ACN = acetonitrile; OctOH = octanol; BuOH = butanol; EtOH = ethanol; MeOH = methanol).

Table 1S. PMI-COOH absorption and emission maxima, quantum yields (QY) and decay times (τ) in different organic solvents. The weighted contributions α are given in the case of multiexponential decays at the emission maximum. The solvent properties (dielectric constant ε and refractive index n) are also given.

Solvent	ε	n	Abs. max. (nm)	Em.max. (nm)	QY	τ (ns)
Methylcyclohexane	2.02	1.422	508	528	0.85	3.6
Dioxane	2.22	1.422	513	549	1	4.1
Toluene	2.40	1.494	515	545	0.93	4
Diethylether	4.20	1.350	509	542	1	4.2
Tetrathydrofuran	7.60	1.407	513	555	0.82	4.2
Acetone	20.60	1.356	509	570	0.85	4.3
Acetonitrile	35.90	1.342	509	578	0.86	4.4
Octanol	10.30	1.429	515	579	0.87	4 0.537 (α<0)*
Butanol	17.50	1.397	514	591	0.74	3.8 0.156 (α<0)*
Ethanol	24.60	1.359	512	593	0.73	3.8 0.042 (α<0)*
Methanol	32.70	1.327	512	597	0.69	3.8 0.015 (α<0)*
Water	80.00	1.333	502	746	0.04	3 (α=0.56) 0.854 (α=0.37) 0.131 (α=0.07)

* The contribution of this decay time is essentially 0 at the emission maximum and negative at long wavelengths (no more than 5%).

A Lippert plot was constructed in order to estimate the sensitivity of the excited state energy of PMI-COOH to the solvent polarity (figure 2S, left). This represents the dependence of the Stoke's shift of the dye on the solvent polarity parameter Δf:

$$\Delta f = \frac{\varepsilon - 1}{2\varepsilon + 1} - \frac{n^2 - 1}{2n^2 + 1},$$

where: ε - dielectric constant of the solvent; n – refractive index of the solvent.

When the solvent polarity parameter Δf is larger than 0.15, the data points fall on two straight lines, one for diethylether, tetrahydrofuran, acetone and acetonitrile, and another one for alcohols. Both lines have similar slopes: 7850 ± 506 and 8031 ± 730, allowing the calculation of the difference between the values of the dipole moment in the ground and the excited state of PMI-COOH using the formula (2):

$$Slope = \frac{\Delta \nu}{\Delta f} = \frac{2\left(\mu_E - \mu_g\right)^2}{4\pi\varepsilon_0 hca^3},$$

where: $\Delta\nu$ – Stoke's shift in wavenumbers (cm^{-1}); Δf – solvent polarity parameter; μ_E – dipole moment of the excited state; μ_g – dipole moment in the ground state; ε_0 – permittivity of vacuum (8.85×10^{-12} C^2 N^{-1} m^{-2}); h – Planck's constant (6.63×10^{-34} J s); c – velocity of light (3×10^8 m s^{-1}); a – radius of the spherical cavity in which the fluorophore is contained. The solvent accessible volume of the molecule calculated from the geometry optimization program AMPAC is 1394 $Å^3$, giving an a value of 6.9 Å. The change in the dipole moment upon excitation for this dye ($\mu_E - \mu_g$) was found to be 16 D (Debye), a value which is comparable to those obtained for other fluorophores (2).

The data obtained for MCH, toluene and dioxane do not fit on the linear plot together with the other solvents. In the case of toluene and dioxane, this can be due to the fact that

they have a stronger solvating power than indicated by their *Δf* values. However, in the representation on the empirical scale $E_T(30)$, where these effects have the same extent for the $E_T(30)$-compound and for the investigated molecule, all the tested solvents except alcohols fall on the same straight line (figure 2S, right).

The fact that the data for alcohols fit on a different line compared to the other solvents on both Lippert plot and $E_T(30)$ representation (figure 2S) can be due to the fact that formation of a hydrogen bond is possible between the –OH group of alcohols and the O atoms of the fluorophore. Because the other solvents (diethylether, tetrahydrofuran, acetone and acetonitrile) can also accept the hydrogen from the –COOH group of the fluorophore, but the behavior of the chromophore follows the expected trend, we suggest that the hydrogen bonds which are formed in alcohols and influence the fluorophore properties are more probably located on the imide part. However, we expect this process to be irrelevant in lipid membranes, as long as the imide part has more chances to be located in the middle of the bilayer, where hydrogen donating groups are not present.

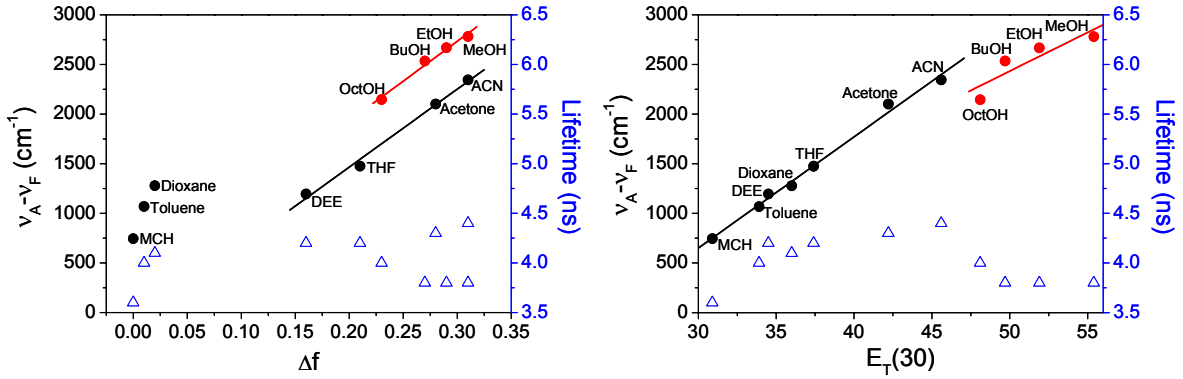

Figure 2S. Two representations of the Stoke's shift of PMI-COOH as a function of solvent polarity: Lippert plot (*left*) and $E_T(30)$ scale (*right*). The variation of the PMI-COOH lifetime is also represented (blue triangles).

The absorption spectrum of PMI-COOH in water shows a shoulder at wavelengths longer than 550 nm, while the maximum is hypsochromically shifted compared to the other solvents. Moreover, the fluorescence quantum yield is very much reduced, so there is practically no fluorescent emission of PMI-COOH in water. The decay of the fluorescence intensity is multiexponential, showing quenched components compared to the other solvents. The combination of these results suggests an extensive aggregation of PMI-COOH in water. The simultaneous observation of a red and a blue shifted maximum in the absorption spectrum suggests either that aggregates with a broad distribution of packing geometry are formed, or that the transition dipoles of neighboring molecules are not parallel in the aggregate.

In order to explore more in depth the aggregation process, mixtures of dioxane/water and tetrahydrofuran (THF)/water were tested. Figure 3S and tables 2S and 3S demonstrate that the situation is different for the two types of mixtures. In the case of dioxane/water mixtures, the shape of the absorption spectrum changes only when 90% water is present, with a blue shift of the absorption maximum (figure 3S). By increasing the water proportion in the mixture, the emission spectrum becomes broader, with a maximum shifted to wavelengths longer than 600 nm, while the fluorescence intensity decreases (figure 3S). These changes are accompanied by a gradual decrease in the fluorescence quantum yield (table 2S). The fluorescence intensity decay changes from a monoexponential curve in pure dioxane to a

multiexponential curve when 65% water or more is added. In the latter case, both shorter and longer components compared to the decay time of the monomer are present.

For the THF/water mixtures, the absorption spectrum clearly shows the presence of a new band above 550 nm when 80% water is added in the mixture (figure 3S). In THF plus 90% water, this band changes and the spectrum is similar to the one recorded for PMI-COOH in water. An abrupt decrease of the fluorescence quantum yield (table 3S) and of the fluorescence intensity is observed for PMI-COOH from the THF mixture containing 65% water to the THF mixture containing 80% water, with the emission maximum shifting above 600 nm. In the latter case, the fluorescence decay becomes multiexponential, but only components with a shorter decay time compared to the monomer lifetime are observed (table 3S).

The multiexponential behavior of the fluorescence decay curves in dioxane/water and THF/water mixtures is considered to be due to the formation of PMI-COOH aggregates. The observation of both shorter and longer components compared to the decay time of PMI-COOH lead to the conclusion that the molecules can aggregate in organic solvents in different geometries (parallel, antiparallel or at different angles). The decay time values of the aggregates are probably depending more on the position the molecules inside the aggregate than on the polarity of the environment, as suggested by the different decay time values observed in mixtures of similar polarity (tables 2S and 3S).

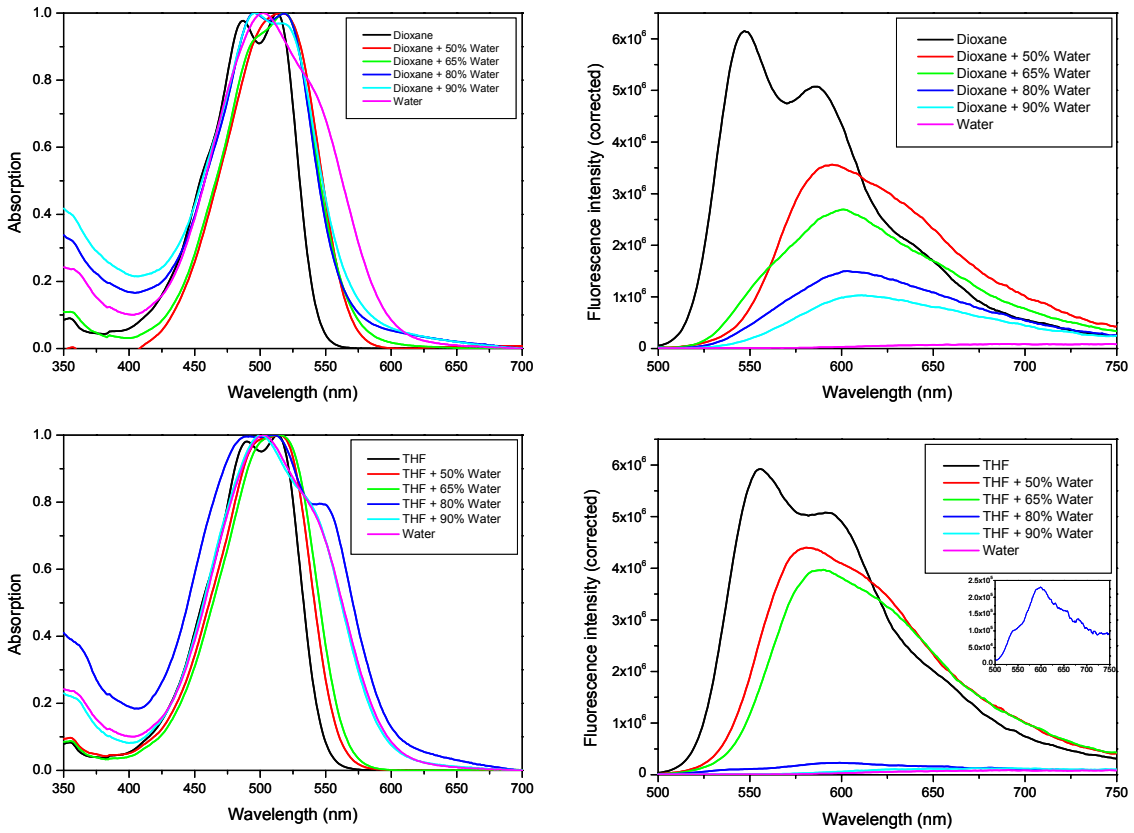

Figure 3S. Absorption (*left*) and emission spectra (*right*) (excitation at 488 nm) of PMI-COOH in mixtures of dioxane/water and tetrahydrofuran (THF)/water. The absorption spectra were normalized for a better visualization of the shape changes. The corrected emission spectra were not normalized, in order to make visible the decrease of the emission intensity after increasing the water proportion in the mixture. The inset in the bottom panel (*right*) shows the emission spectrum of PMI-COOH in THF with 80% water.

Table 2S. PMI-COOH absorption and emission maxima, quantum yields (QY) and decay times (τ) in mixtures of dioxane and water. The weighted contributions α are given in the case of multiexponential decays at the emission maximum. The dielectric constants ε of the mixtures were taken from ref. 3 and the refractive indices n were experimentally determined using an Abbe refractometer.

Solvent	ε	n	Abs. max. (nm)	Em.max. (nm)	QY	τ (ns)
Dioxane	2.22	1.422	513	549	1	4.1
Dioxane + 50% Water	35.90	1.384	516	593	0.85	3.8 0.245 (α<0)*
Dioxane + 65% Water	48.90	1.369	518	601	0.67	8.5 (α=0.34) 2.9 (α=0.62) 0.877 (α=0.04)
Dioxane + 80% Water	61.90	1.354	496	603	0.40	9.9 (α=0.66) 3.3 (α=0.24) 0.741 (α=0.08) 0.165 (α=0.02)
Dioxane + 90% Water	70.30	1.344	496	609	0.31	10 (α=0.64) 3.4 (α=0.27) 0.756 (α=0.07) 0.130 (α=0.02)

* The contribution of this decay time is essentially 0 at the emission maximum and negative at long wavelengths (no more than 5%).

Table 3S. PMI-COOH absorption and emission maxima, quantum yields (QY) and decay times (τ) in mixtures of THF and water. The weighted contributions α are given in the case of multiexponential decays at the emission maximum. The dielectric constants ε of the mixtures were taken from ref. 4 and the refractive indices n were experimentally determined using an Abbe refractometer.

Solvent	ε	n	Abs. max. (nm)	Em.max. (nm)	QY	τ (ns)
THF	7.60	1.407	513	555	0.82	4.2
THF + 50% Water	54.60	1.377	514	583	0.91	4 0.543 (α<0)*
THF + 65% Water	59.00	1.366	514	592	0.86	3.9 0.484 (α<0)*
THF + 80% Water	73.10	1.352	510	601	0.15	4 (α=0.87) 0.739 (α=0.09) 0.175 (α=0.04)
THF + 90% Water	76.40	1.343	500	692	0.06	3.4 (α=0.27) 0.657 (α=0.52) 0.185 (α=0.21)

*The contribution of this decay time is essentially 0 at the emission maximum and negative at long wavelengths (no more than 5%).

Aggregation of PMI-COOH in the gel phase. Based on the considerations discussed for the organic solvents, several experimental observations lead to the idea that a large fraction of the

PMI-COOH molecules form aggregates in the gel phase. First, there is a similar shape of the PMI-COOH excitation spectrum in the gel phase and the absorption spectrum in water. Second, the maximum of the emission spectrum in the gel phase is shifted to wavelengths longer than 600 nm, the spectrum is broad, lacking vibrational structure, and the fluorescence intensity is very low. Third, an important contribution of a long decay time (12 ns) was found in the time-resolved measurements. A similar change in the absorption spectrum and an increase of the decay time was found for a related chromophore, perylene diimide, when two molecules are fixed by chemical bonds with the aromatic planes parallel to each other (5-7). However, a final proof to demonstrate the aggregation in this lipid phase would be to observe the spectral and decay time modifications after reducing the concentration of the dye in the bilayer. Obviously, this will reduce the probability of aggregation. The experiments were done with three dye/lipid ratios: 1/500, 1/1000 and 1/2000. Although the excitation and emission spectra do not significantly differ in the three situations (figure 4S), the contributions of the PMI-COOH decay times show a clear trend (figure 5S). At 560 nm, the contribution of the long component (12 ns) decreases from 25% to 20% and 2.5% as the dye/lipid ratio decreases. On the other hand, the contribution of the characteristic decay time for the monomer (4.7-4.9 ns) increases from ≈ 65% for the ratio 1/500 to ≈ 85% for the ratio 1/2000 at 560 nm. It is significant to note that for the dye/lipid ratio 1/2000, the contribution of the monomer emission dominates even at longer wavelengths (610 nm). This set of experiments demonstrates that we can confidently attribute the long decay time that was found in all the lipid phases to the dye aggregates in the membrane. The fact that the long component has different values in the Ld, Lo and gel phases is probably due to the fact that different types of aggregates can be formed, as proved by time-resolved measurements in organic solvents.

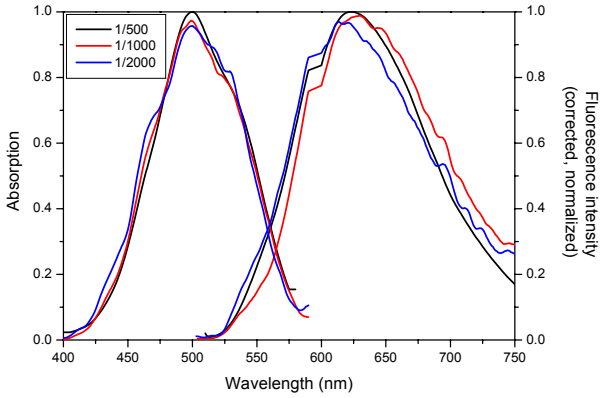

Figure 4S. Excitation and emission spectra of PMI-COOH embedded in the gel phase in three dye/lipid ratios: 1/500, 1/1000 and 1/2000.

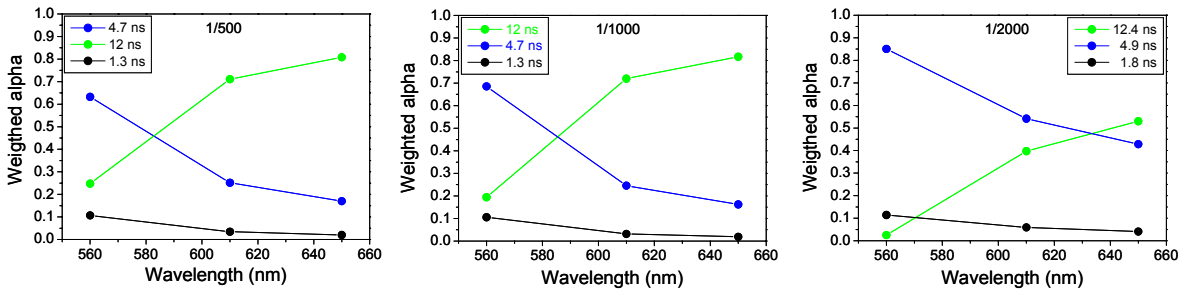

Figure 5S. Contributions of the PMI-COOH decay times in the gel phase for different dye/lipid ratios: 1/500, 1/1000 and 1/2000.

Converting arrival times to lifetimes. In order to avoid aggregation of PMI-COOH, which introduces undesired complex photophysics, we worked with a very low concentration of PMI-COOH for the GUVs (lipid:dye ratio 125000:1) and for the Jurkat cells (4×10^{-9} M). At this ratio, there is no aggregation and the decay times become monoexponential for the different phases, meaning 4.7 ns for both the Ld and the gel phase, and 6.5 ns for the Lo phase. As a result of the very low concentration of PMI-COOH, the number of the photons in each pixel in the FLIM image is quite limited (less than 100 photons/ADC channel in a pixel). Furthermore, the number of ADC channels used to record the FLIM images was 256. For this reason, it was not possible to do the same analysis which was performed for the bulk measurements with high quality data (10000 photons in the maximum and 4096 ADC channels). Therefore, instead of directly deconvoluting the decay curve of each pixel, we measured the average arrival time of the photons in each pixel, and converted it to the corresponding lifetime by taking into account the instrumental response function. This analysis scheme is robust for decays with a low number of data points, and equivalent to deconvolution analysis in the case of a single exponential decay curve. An example of the estimation of average arrival time is shown in figure 6S. The procedure to convert average arrival time to lifetime is as follows. The measured instrumental response function (figure 6S A) is convolved with an exponential function (figure 6S B), and the average arrival time is estimated.

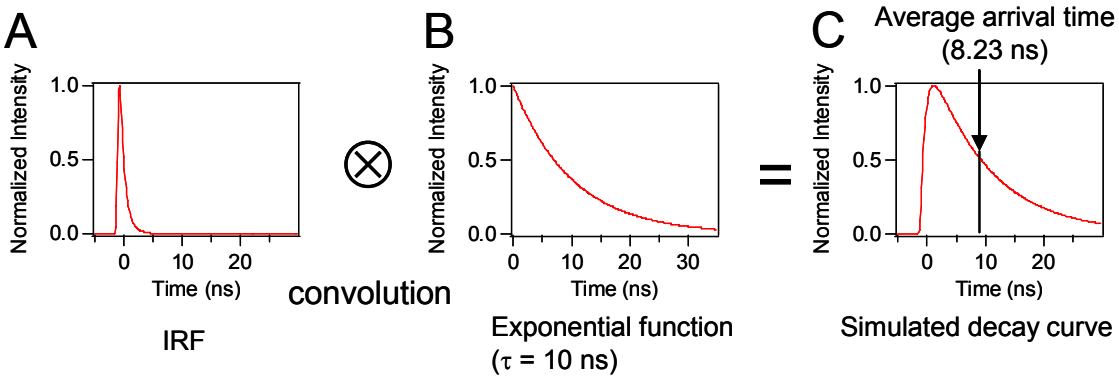

Figure 6S. Schematic representation for the estimation of average arrival times. The instrumental response function (IRF) is convolved with an exponential function with a certain decay time (10 ns in this example). The average arrival time is estimated from the simulated convolved curve by calculating the expected value of the arrival time.

This estimation was done for lifetimes ranging from 0 to 20 ns in steps of 0.1 ns and a calibration curve for the conversion of average arrival time to lifetime was generated (figure 7S). Using this calibration curve, the average arrival time of each pixel is converted to lifetime by extrapolation, and the average arrival time images (figure 8S A) are converted to FLIM images (figure 8S B).

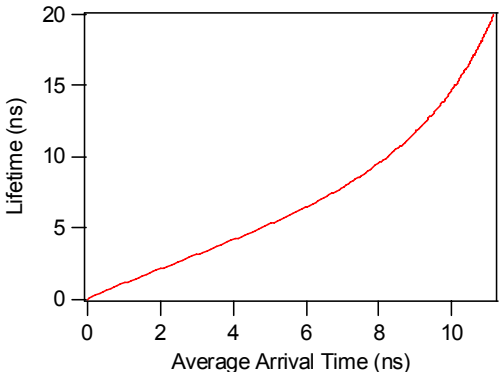

Figure 7S. Calibration curve for conversion from average arrival time to lifetime.

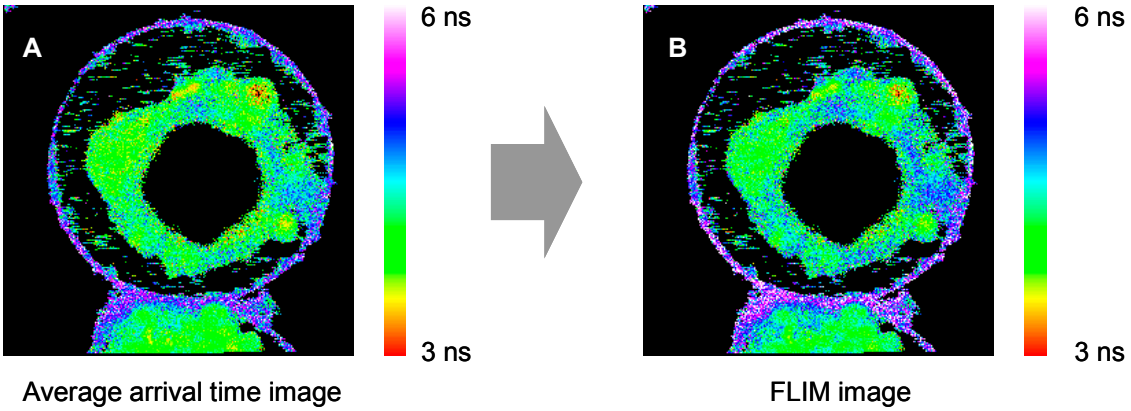

Figure 8S. An example of the conversion from average arrival time image to FLIM image.

References

1. Baruah, M., W. Qin, C. Flors, J. Hofkens, R. A. L. Vallée, D. Beljonne, M. Van der Auweraer, W. M. De Borggraeve, N. Boens. Solvent and pH dependent fluorescent properties of a dimethylaminostyryl borondipyrromethene dye in solution. 2006. *J. Phys. Chem. A* 110:5998-6009.
2. Lakowicz, J. R. 1999. Principles of fluorescence spectroscopy, 2nd ed., Kluwer Academic / Plenum Publishers, New York, NY, pp. 185-236.
3. Martel, R.W., and C. A. Kraus. 1955. The association of ions in dioxane-water mixtures at 25°. *Proc. Natl. Acad. Sci. USA* 41:9-20.
4. Kumbharkhane, A. C., S. N. Helambe, M. P. Lokhande, S. Doraiswamy, and S. C. Mehrotra. 1996. Structural study of aqueous solutions of tetrahydrofuran and acetone mixtures using dielectric relaxation technique. *Pramana J. Phys.* 46:91-98.
5. van der Boom, T., R. T. Hayes, Y. Zhao, P. J. Bushard, E. A. Weiss, and M. R. Wasielewski. 2002. *J. Am. Chem. Soc.* 124: 9582-9590.
6. Ahrens, M. J., L. E. Sinks, B. Rybtchinski, W. Liu, B. A. Jones, J. M. Giaimo, A. V. Gusev, A. J. Goshe, D. M. Tiede, and M. R. Wasielewski. 2004. *J. Am. Chem. Soc.* 126: 8284-8294.
7. Hofkens, J., T. Vosch, M. Maus, F. Köhn, M. Cotlet, T. Weil, A. Herrmann, K. Müllen, and F. C. De Schryver. 2001. *Chem. Phys. Lett.* 333:255-263.